Effect of the diesel injection timing and the pilot quantity on the combustion characteristics and the fine-particle emissions in a micro-diesel pilot-ignited natural-gas engine

Lei Zhou, Yi-Fu Liu, Chen-Bo Wu, Lu Sun, Long Wang, Ke Zeng and Zuo-Hua Huang

Proceedings of the Institution of Mechanical Engineers, Part D: Journal of Automobile Engineering 2013 227: 1142
originally published online 13 March 2013
DOI: 10.1177/0954407013480452

Original Article

Institution of MECHANICAL ENGINEERS
Journal of AUTOMOBILE ENGINEERING

Proc IMechE Part D:
J Automobile Engineering
227(8) 1142–1152

DOI: 10.1177/0954407013480452
pid.sagepub.com
SAGE

Effect of the diesel injection timing and the pilot quantity on the combustion characteristics and the fine-particle emissions in a micro-diesel pilot-ignited natural-gas engine

Lei Zhou, Yi-Fu Liu, Chen-Bo Wu, Lu Sun, Long Wang, Ke Zeng and Zuo-Hua Huang

Abstract

Natural gas is a potential alternative to conventional liquid fuels for utilization in automotive internal combustion engines. Its utilization can significantly reduce the levels of nitrogen oxide and particulate matter emissions from dual-fuel diesel/natural-gas engines. However, this reduction in the particulate matter emissions may induce an increase in the quantity of particles of smaller size, which are harmful to human health. The engine parameters, namely the diesel injection timing and the pilot quantity directly, affect the homogeneity of the fuel–air mixture, the spatial distribution of initial ignition centres and the quantity of initial ignition centres. In this paper, the effects of these two engine parameters on the combustion and the particle emission characteristics of micro-diesel pilot-ignited natural-gas fuel are investigated. The combustion parameters were calculated from the cylinder pressure data. An electrical low-pressure impactor was employed to measure the particle number concentration and particle size distribution. Experimental results indicate that the ignition delay period is prolonged and the particle number concentration progressively increases with advance of the injection timing, while the particle mass concentration undergoes a steady decrease and then a rapid increase. On the other hand, increasing the pilot diesel quantity can shorten the ignition delay period and enhance the burning rate. Meanwhile, the particle mass concentration increases evidently but the particle number concentration decreases unexpectedly. It should be noted that the total number of fine particles is sensitive to advancing injection and decreasing pilot mass, especially above the 20° crank angle before top dead centre injection timing and below the basic pilot mass.

Keywords

Natural gas, diesel, pilot, fine particles, combustion, injection timing, pilot mass

Date received: 1 July 2012; accepted: 31 January 2013

Introduction

With increasing concern about fossil fuel shortages, soaring oil prices and severe environmental issues, the study of alternative fuels has become one focus of recent vehicle engine studies. Natural gas has been considered to be one of the alternative fuels for internal combustion engines with the highest potential owing to its relatively rich reserves, lower prices and better emissions. Additionally, the diversity of global energy supply also provides an opportunity for natural-gas fuel application in vehicle engines. Therefore, natural gas has been extensively used in public and commercial transportation vehicles in cities.

Natural-gas engines consist of natural-gas spark ignition (NGSI) engines and natural-gas compression ignition (NGCI) engines. Compared with NGSI engines, NGCI engines can operate at higher compression ratios and yield higher brake thermal efficiencies and better fuel economies because natural-gas fuel has a relatively higher octane number and a better anti-knock property. NGCI engines primarily include natural-gas homogeneous charge compression ignition

School of Energy and Power Engineering, Xi'an Jiaotong University, Xi'an, People's Republic of China

Corresponding author:
Ke Zeng, Xi'an Jiaotong University, Xianning Road, Xi'an 710049, People's Republic of China.
Email: zengke131.xjtu@gmail.com

(NG-HCCI) engines and dual-fuel natural-gas premixed charge compression ignition (NG-PCCI) engines. Additionally, a new-efficient high-pressure direct-injection system,[1,2] which uses a dual-needle dual-actuator fuel injector to inject directly both diesel and natural gas into the chamber, has been studied in order to modify the performance and emissions of diesel pilot natural-gas engines.

The homogeneous charge compression ignition (HCCI) combustion strategy is a combustion method of autoigniting a super-lean mixture through compression using the piston alone, without any external ignition source. For NG-HCCI engines, because of the relatively high autoignition temperature of natural gas and the lower density of gas fuel, NG-HCCI engines generally require higher compression ratios and intake charge heating and even need the intake and exhaust valve timing to be changed or hot exhaust gas recirculation (EGR) to be utilized to achieve stable operation.[3–6] NG-HCCI engines, in contrast, can produce better fuel brake specific fuel consumptions and extremely low nitrogen oxide (NO_x) emissions; however, several tough challenges such as control of the ignition phase, unstable combustion, load fluctuations and limits of the operating range still need to be confronted at present.

Dual-fuel NG-PCCI combustion, compared with NG-HCCI combustion, is easier to achieve despite the need to add one natural-gas fuel supply system.[7] Most dual-fuel NG-PCCI engines are modified from conventional diesel engines by inducting the natural gas into the combustion chamber via the intake manifold, while maintaining the original diesel injection (in diesel pilot NG-PCCI engines). A relatively small quantity of diesel fuel (1–5% by energy[8]) is injected into the chamber as the only ignition resource to pilot ignite the lean natural-gas–air mixture, while the power output of the engine is adjusted through the amount of natural gas.

Most diesel pilot NG-PCCI studies have mainly focused on the diesel pilot natural-gas engine performance, combustion mechanism, combustion process characteristics and exhaust emissions characteristics. Using an optical engine, Yao et al.[9] revealed the ignition mechanism of the diesel pilot natural gas. They found that the ignition location of the diesel and natural gas was more dispersed and was closer to the cylinder wall than that of pure diesel. Papagiannakis et al.[7,10] investigated the effect of the diesel and natural-gas percentages on the combustion and the emission characteristics. The results indicated that the ignition delay period and the total combustion duration are prolonged with increasing the natural-gas percentage. Importantly, the diesel pilot NG-PCCI combustion mode can significantly reduce the NO_x emissions and the particulate matter (PM) emissions, but it is at the cost of the increasing the hydrocarbon (HC) emissions and the carbon monoxide (CO) emissions. In order to resolve these problems, Krishnan et al.[11,12] and Srinivasan et al.[8,13–15] utilized several methods such as enhancing the intake charge temperature, increasing slightly the diesel pilot quantity, advancing the injection timing and utilizing the EGR strategy. Eventually, the total HC and CO emissions were controlled to acceptable levels, while maintaining lower NO_x levels than the US Environmental Protection Agency 2007 mandates.[8] Meanwhile, the diesel pilot NG-PCCI engine can obtain a matching diesel engine efficiency or even a higher efficiency under experimental conditions.

PM emissions have been found to have adverse effects on human health, especially for particles of smaller size, since they have the potential to penetrate deep into the lungs and to dissolve in the bodily fluids.[16–18] Automotive engines are a major source of fine particles (an aerodynamic particle diameter D_p of less than 2.5 μm) and ultrafine particles ($D_p < 0.1$ μm) emitted into the atmosphere. Therefore, the number concentration of smaller particles from engines has continued to attract more attention recently. A dual-fuel premixed charge compression ignition (PCCI) combustion strategy has been considered as an effective method to reduce the particle mass by adjusting the engine parameters.[19–21] However, several research results suggested that this reduction in the particle mass through using the PCCI combustion strategy may be accompanied by an increase in the number of smaller particles.[20,22,23] For diesel pilot NG-PCCI engines, the previous PM studies were focused primarily on reducing the particle mass emissions. There have still not been a sufficient number of these studies in the extensive investigations on particle number variations and distributions. Therefore, this present study further expands upon previous research and mainly concerns the variations in the number of smaller particles.

The basic parameters of diesel pilot NG-PCCI engines, namely the diesel injection timing and the diesel pilot quantity (pilot mass), significantly affect the particle number concentration and the particle size distribution. These parameters directly determine the quantity of initial ignition kernels, the spatial distribution of initial ignition centres and the homogeneity of the total charge. The variations in the distribution of initial ignition kernels, the quantity of initial ignition kernels and the homogeneity of the total charge can lead to variations in the initial burning rate, the formation of particles and the oxidation of particles, eventually producing different particle number concentrations and size distributions. Therefore, the purpose of this study is to investigate the effects of the diesel injection timing and the diesel pilot mass on the combustion characteristics and the emission characteristics (in particular, the emissions of smaller particles).

Experimental set-up and procedure

Test engine

The experimental set-up is shown in Figure 1. A single-cylinder four-stroke direct-injection compression ignition engine was employed and its intake system was

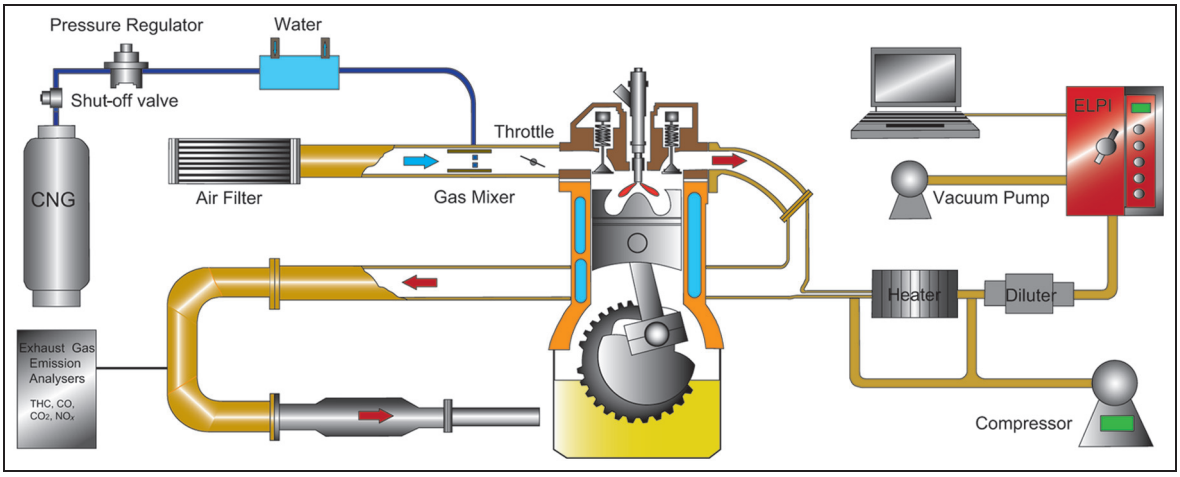

Figure 1. Schematic diagram of the experimental set-up.
CNG: compressed natural gas; THC: total hydrocarbon; CO: carbon monoxide; CO_2: carbon dioxide; NO_x: nitrogen oxides; ELPI: electrical low-pressure impactor.

modified to satisfy the natural-gas supply. The specifications of the engine are listed in Table 1. The natural-gas supply system is composed of a compressed natural-gas fuel tank, a pressure regulator and one natural gas–air mixer. A step motor was used to control the amount of natural-gas flow. The pilot diesel mass was controlled manually to obtain stable ignition resources, while the air-to-fuel ratio was monitored using a HORIBA MEXA-700λ instrument with a measurement accuracy of 1%.

Table 1. Engine specifications.

Engine type	Single-cylinder four-stroke direct-injection engine
Combustion chamber	ω type
Bore	100 mm
Stroke	115 mm
Displacement	903 cm^3
Compression ratio	18:1
Diesel fuel injector	Four holes, 0.3 mm diameter
Injection pressure	20 MPa
Rated power/speed	10 kW
Rated speed	2000 r/min
Primary fuel	Natural gas
Gas fuel supply	Intake manifold

Experimental instruments

The experimental system was instrumented to measure the in-cylinder pressure, the air consumption and the fuel consumption as well as the exhaust emissions (HC, CO, carbon dioxide (CO_2), NO_x and PM). The cylinder pressure data were obtained with a Kistler 6117B piezoelectric pressure transducer and recorded at a crank angle (CA) of 0.2° for 200 consecutive completed cycles to analyse the combustion parameters. The intake air mass flow was measured with a thermal mass flow meter, and the consumptions of the natural gas and pilot diesel mass were acquired using two high-precision electronic balances both with accuracies of ±0.1 g.

The exhaust gas emissions were sampled directly from the exhaust pipe. The total HC, CO and CO_2 emissions were measured with a HORIBA MEXA-5541JA exhaust analyser with accuracies of ±12 ppm, ± 0.06% and ± 0.5% respectively, while the NO_x emissions were measured with a MEXA-720 NO_x analyser with an accuracy of ± 30 ppm.

The particle number concentration and size distribution were measured using an electrical low-pressure impactor (ELPI) analyser with an extra filter stage. The ELPI used was similar to that in earlier work reported by other researchers.[24–27] This measurement with the ELPI covered a particle size from 7 nm to 10 μm with 12 filter stages. The detailed process and principle of particle measurement have been described in the paper by Tsolakis et al.[25] To avoid overloading the ELPI's electrometer, the exhaust gas was diluted with clean air using a two-stage diluter manufactured by Dekati. Two diluters are used with constant dilution ratios of 8.43 and 8.45 respectively. The dilution ratio is kept constant for all tests to provide the basis for the discussion of particle emissions. In addition, to eliminate the unexpected particle condensation and nucleation during dilution, the first stage of the diluter is heated to 200 °C and the second stage of the diluter operates at ambient temperature.

Since the aerodynamic particle diameters in diesel pilot NG-PCCI engines are primarily in the range less than 1 μm (i.e. the PM1 range), therefore, the present study focuses on only smaller particles in the PM1 range. The data from stage 1 to stage 8 were recorded. By assuming a particle density of unity and weighting the distributions by D_p^3, the distribution of the particle mass versus the size was obtained.[26] In fact, the shapes of the particles in diesel pilot natural-gas engines are nearly spherical.[28]

Table 2. Main properties of diesel fuel and natural gas.

Parameter (units)	Value for the following	
	Diesel fuel	Natural gas
Low heating value (MJ/kg)	43.1	48.6
Cetane number	52.5	—
Octane number	—	130
Autoignition temperature (°C)	250	650
Stoichiometric air-to-fuel ratio	14.69	17.2
Sulphur content (ppm)	< 50	—
Components	—	96.16% CH_4, 2.5% CO_2, etc.

Experimental fuels

In the present study, the diesel fuel used was an ultra-low sulphur (less than 50 ppm) diesel fuel, and the natural gas was a typical commercial fuel. The main properties of the diesel fuel and the natural gas are shown in Table 2.

Experimental procedure

For the diesel pilot NG-PCCI engine, two concepts (the basic pilot mass and the minimum pilot mass) need to be defined before discussion. At a given engine speed, diesel fuel is introduced as the only participator to offset the engine mechanical losses. The power output is zero without any natural-gas injection and this corresponding diesel consumption quantity is called the basic pilot mass.[7] Diesel fuel and natural gas participate commonly in the combustion to offset approximately the engine mechanical losses at a given engine speed, and the corresponding diesel consumption quantity is the minimum pilot mass.

During the whole experimental process, the engine was run at three speeds (1200 r/min, 1600 r/min and 2000 r/min, three lower brake mean effective pressure (BMEP) levels (0.14 MPa, 0.28 MPa and 0.42 MPa), five injection timings and three pilot masses (minimum pilot mass, basic pilot mass and 150% basic pilot mass). In all the cases examined, the lubricating oil temperature and the cooling-water temperature were maintained at 70 °C and 80 °C respectively. Fuel consumptions were recorded over 5 min periods, and measurement was repeated three times in each engine steady state condition. If the deviation of the measurement data was beyond the predefined limit (3%), the measurement was conducted again.

Combustion parameters

A thermodynamic model is used to calculate the combustion process parameters. The model neglects the leakage through the piston rings,[29] and thus the cylinder energy conservation can be expressed as

$$\frac{\mathrm{d}Q_B}{\mathrm{d}\varphi} = p\frac{C_p}{R}\frac{\mathrm{d}V}{\mathrm{d}\varphi} + \frac{C_V V}{R}\frac{\mathrm{d}P}{\mathrm{d}\varphi} + mT\frac{\mathrm{d}C_V}{\mathrm{d}\varphi} + \frac{\mathrm{d}Q_w}{\mathrm{d}\varphi} \quad (1)$$

where the heat transfer rate is given by

$$\frac{\mathrm{d}Q_w}{\mathrm{d}\varphi} = h_c A(T - T_w) \quad (2)$$

The heat transfer coefficient h_c uses the correlation formula given by Woschni.[30] Properties such as the heat capacity at constant pressure and the heat capacity at constant volume for species can be obtained from the National Aeronautics and Space Administration database.[31,32] Because of the unknown mass fraction burned at every time step, a simple iterative method is introduced to calculate the thermodynamic properties of the mixture, which includes the burned and the unburned parts. Using the above formulas and the cylinder pressure data, the heat release rate and combustion parameters can be calculated.

The following combustion parameters are defined to facilitate the analysis of the combustion process. The ignition delay period Δ_{IGN} is defined as the time interval from the diesel fuel injection timing to the onset of ignition timing. The total combustion duration Δ_{COM} is the duration from the start of ignition to the end of combustion. $\Delta_{50\%}$ is the 50% mass burned CA relative to the compression top dead centre (TDC)[14]. The CA of the centre of the heat release curve is determined by the formula

$$\varphi_c = \frac{\int_{\varphi_s}^{\varphi_e} (\mathrm{d}Q_B/\mathrm{d}\varphi)\varphi \, \mathrm{d}\varphi}{\int_{\varphi_s}^{\varphi_e} (\mathrm{d}Q_B/\mathrm{d}\varphi) \, \mathrm{d}\varphi} \quad (3)$$

in which φ_s is the CA at the beginning of heat release and φ_e is the CA at the end of heat release.

Results and discussion

In this study, the diesel injection timing and the pilot mass are independently analysed and evaluated for combustion and emissions in different engine operation conditions.

Effect of the injection timing on the combustion and the gaseous emissions

Figure 2 shows the effects of the injection timing on the combustion parameters. The results show that, under a constant micro-diesel pilot mass, Δ_{IGN} is prolonged continuously with advancing injection timing from 10° CA BTDC to 30° CA BTDC, while the $\Delta_{50\%}$ curve evidently decreases. The variations in Δ_{IGN} and $\Delta_{50\%}$ can be mainly attributed to the inconsistent ignition phase caused by the variation in the diesel injection timing.

When the piston moves up at the compression stroke, the cylinder temperature is increased incessantly. If the injection timing is advanced excessively, such as to 30° CA BTDC, this may cause misfire

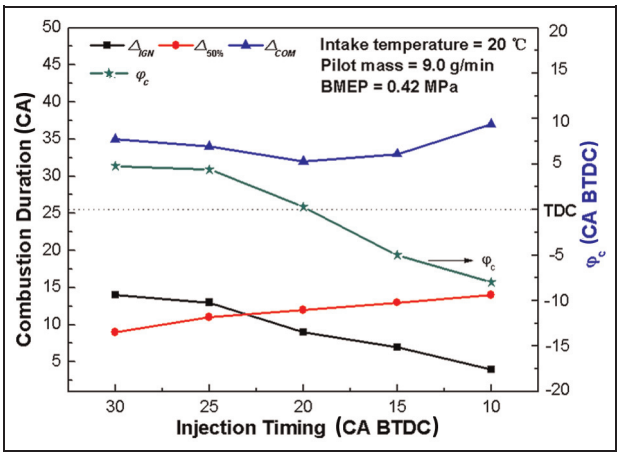

Figure 2. Combustion duration versus injection timing at 1600 r/min engine speed.
CA: crank angle; BMEP: brake mean effective pressure; TDC: top dead centre; BTDC: before top dead centre.

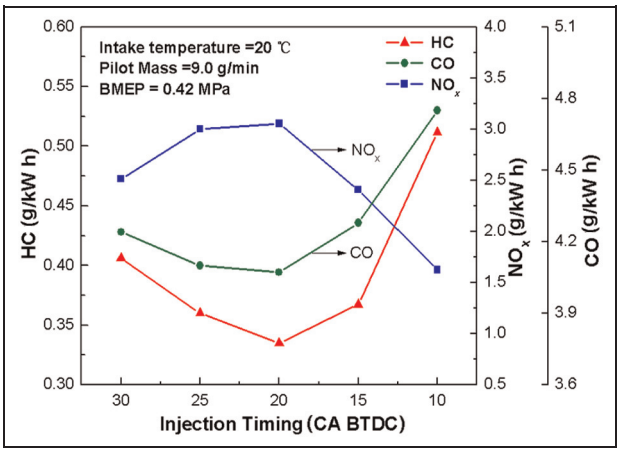

Figure 3. Exhaust HC, CO and NO_x emissions versus injection timing at 1600 r/min engine speed.
BMEP: brake mean effective pressure; HC: hydocarbon; CO: carbon monoxide; NO_x: nitrogen oxides; CA: crank angle; BTDC: before top dead centre.

and partial combustion,[13] since the local in-cylinder temperatures are not sufficiently high to ensure fast diesel evaporation and ignition immediately. Consequently, the residence time of diesel in the cylinder before ignition is increased. Therefore, the longest Δ_{IGN} in Figure 2 appears at 30° CA BTDC. When the injection timing is retarded from 30° CA BTDC to 10° CA BTDC, the in-cylinder temperature of the corresponding injection timing is enhanced gradually, which favours fast ignition and reduces the residence time. Therefore, Δ_{IGN} for the corresponding injection timing is shortened.

A longer Δ_{IGN} allows more time for micro-diesel evaporation, dispersion and mixing with the surrounding natural-gas–air mixture, which results in a multitude of distributed ignition centres throughout the cylinder. These distributed ignition centres produce rapid flame propagation and thus increase the initial burning rate (or heat release rate).[29] Thus, burning 50% charge mass can take a shorter time. Therefore, with retarding the injection timing from 30° CA BTDC to 10° CA BTDC, $\Delta_{50\%}$ increases and the initial burning rate decreases. It should be noted that the CA corresponding to 50% mass burned is close to top dead centre (TDC) and even beyond TDC with retarded injection timing. Correspondingly, the bulk of the combustion process shifts backwards and even occurs in the expansion stroke. This variation leads to a φ_c value (the CA of the centre of heat release) close to the TDC gradually and then far from the TDC, as shown in Figure 2.

The combustion duration presents less variation for the injection timing between 30° CA BTDC and 20° CA BTDC when compared with the injection timing retarded beyond 20° CA BTDC. For the injection timing between 20° CA BTDC and 30° CA BTDC, φ_c is close to the TDC, which implies that heat is released in the higher-temperature zone and thus produces a higher burning rate and a shorter total combustion duration. When the injection timing is retarded beyond 20° CA BTDC, the bulk of the heat release deviates from the TDC and the corresponding total burning rate decreases. Thus the total combustion duration is prolonged.

Figure 3 displays the variations in the total HC, CO and NO_x emissions at different injection timings. The HC and CO emissions decreased between 30° CA BTDC and 20° CA BTDC steadily and then sharply increases between 20° CA BTDC and 10° CA BTDC, reaching a minimum at 20° CA BTDC. Correspondingly, the NO_x emissions exhibit the opposite trend in comparison with the total HC emissions, reaching a maximum at 20° CA BTDC.

For 30° CA BTDC injection timing, as previously mentioned, a longer Δ_{IGN} provides a longer mixing time for diesel–air mixing, thereby causing an over-lean and locally over-homogeneous mixture prior to ignition. This leads to lower local in-cylinder temperatures, which in turn weakens HC and CO oxidation and limits NO_x formation. Therefore, higher HC and CO emissions and lower NO_x emissions are generated. However, for injection timings between 25° CA BTDC and 15° CA BTDC, both the improved initial ignition conditions (the in-cylinder temperature) and the relative concentration heat release (as shown by φ_c in Figure 2) enhance the in-cylinder temperature together during the combustion process. Whereas, when the injection timing is retarded from 15° CA BTDC to 10° CA BTDC, the initial heat release rates are lower, as previously mentioned. Furthermore, the bulk of the heat release occurs in the expansion stroke, as shown by φ_c in Figure 2, resulting in a

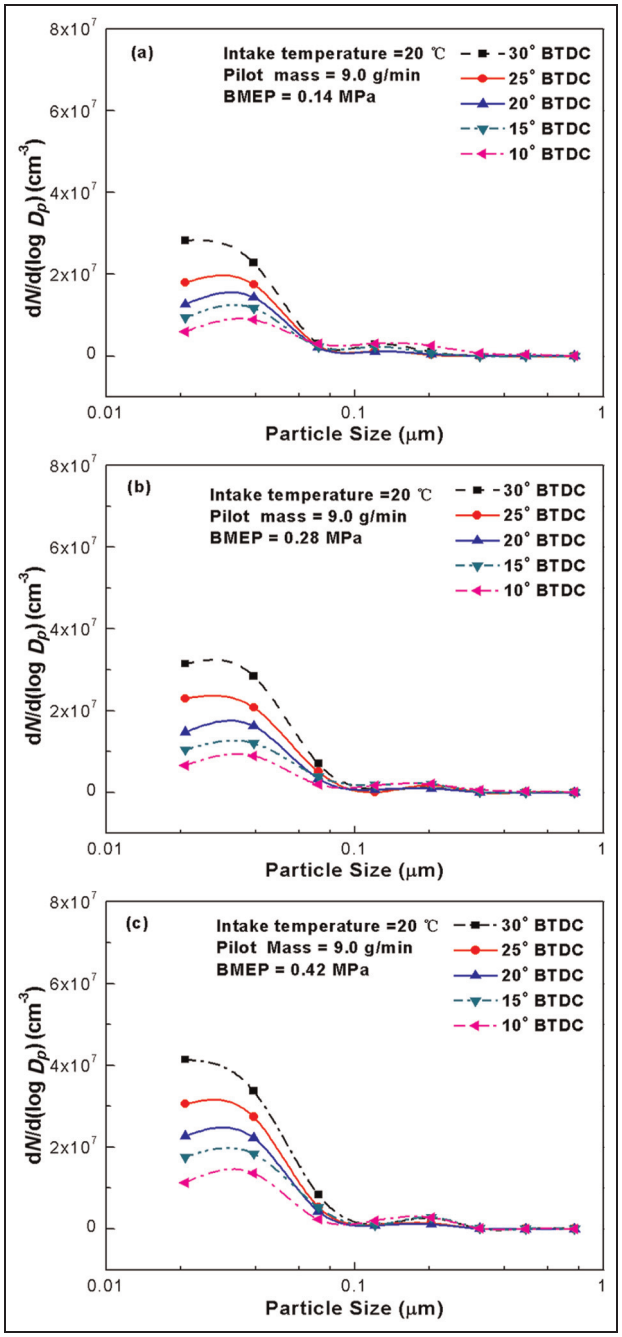

Figure 4. Particle number concentration with respect to the size distribution for various injection timings at 1600 r/min engine speed.
BMEP: brake mean effective pressure; BTDC: before top dead centre.

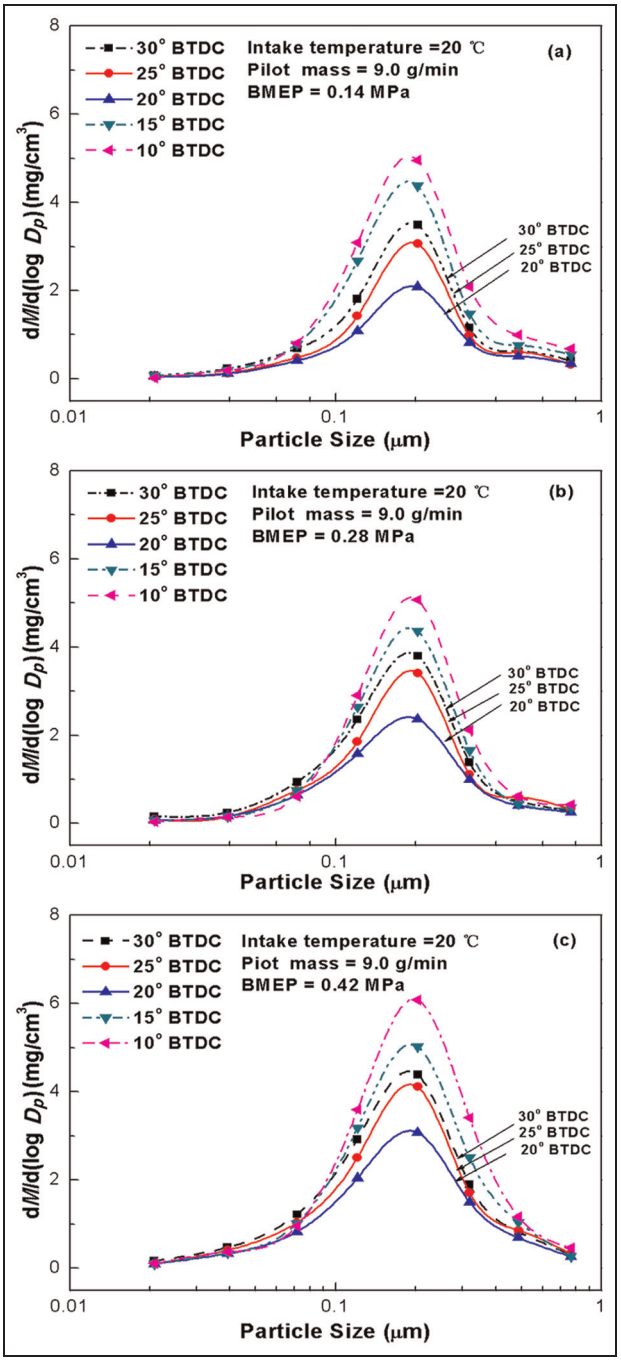

Figure 5. Particle mass concentration with respect to the size distribution for various injection timings at 1600 r/min engine speed.
BMEP: brake mean effective pressure; BTDC: before top dead centre.

lower in-cylinder temperature. Thus, this lower in-cylinder temperature leads to lower NO_x and higher HC and CO emissions.

Effect of the injection timing on the particulate matter emissions

Figures 4, 5 and 6 present the effect of the injection timing on the particle number concentration and the particle mass concentration for different engine operation conditions. They show the same or similar characteristics of the particle emissions at different engine speeds. The effect of the injection timing on the characteristics of the particle emissions is the focus. Therefore, consider, for example, the particle emissions at an engine speed of 1600 r/min. For each engine operating condition, the advance of the injection timing from 10° CA BTDC to 30° CA BTDC results in an significant increase in the number of particles over the entire range of ultrafine particles, as shown in Figure 4. The particle size distribution curves all appear unimodal in shape, and the maximum peak number of

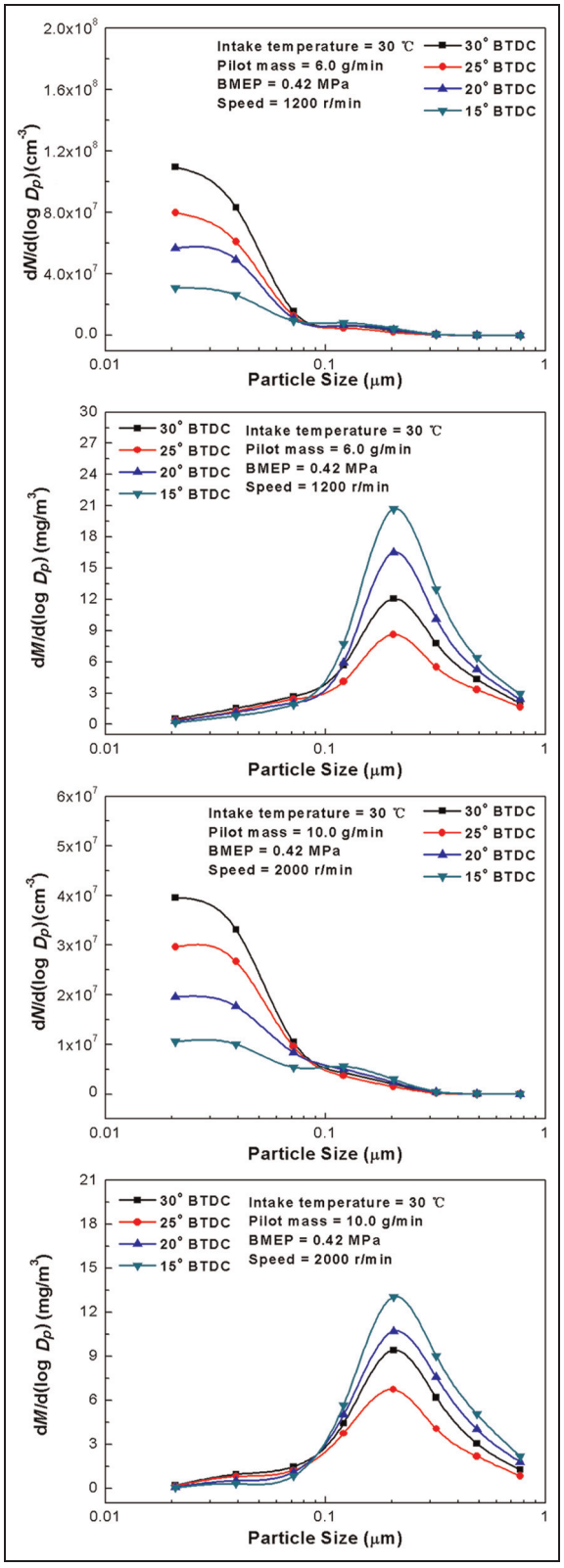

Figure 6. Particle number concentration and particle mass concentration for various injection timings at 1200 r/min and 2000 r/min engine speeds.
BMEP: brake mean effective pressure; BTDC: before top dead centre.

particles is located at a diameter of 0.039 μm. However, as indicated in Figure 5, the particle mass concentration exhibits a sharply decreasing trend from 10° CA BTDC to 20° CA BTDC, and finally a dramatic increase from 25° CA BTDC to 30° CA BTDC. The particle mass distribution peaks at a particle diameter of around 0.2 μm. To explain these variations in the particle number and mass concentrations, the variation in the combustion processes caused by various injection timings is analysed.

For a specific pilot diesel mass, further advanced injection would produce a longer Δ_{IGN} and result in a more homogeneous mixture before ignition. The homogeneous mixture, objectively, can contribute to reducing the possibility that larger particles are formed and to raising the potential that a multitude of smaller particles are generated. Additionally, the lower in-cylinder temperature produced by further advanced injection slows down particle oxidation and thus further increases the number of particles.

When retarding the injection timing from 30° CA BTDC to 20° CA BTDC, although the homogeneity of the mixture is influenced, the total in-cylinder temperature is increased and thus accelerates particle oxidation. As a result, the particle number concentration is reduced sufficiently. However, as the injection timing is retarded from 20° CA BTDC to 10° CA BTDC, both the homogeneity of the mixture and the total in-cylinder temperature are decreased. Consequently, the possible potential for an increase in the amount of smaller particles generated is reduced and particle oxidation is mitigated. Therefore the number of particles is reduced. Nevertheless, this inhomogeneous mixture further aggravates the formation of larger particles. Therefore, the particle mass concentration is increased for injection timings between 20° CA BTDC and 10° CA BTDC.

It must be noted that the particle mass concentration at an injection timing of 30° CA BTDC is higher than that at an injection timing of 20° CA BTDC in Figure 5. This result is not consistent with the previous expectation that advanced injection would create fewer large particles for a given pilot mass. However, the phenomenon that advancing the injection timing might lead to the increase in the particle mass was observed by De Ojeda et al.[33] This discrepancy might be explained by a combination mechanism of PM behaviour. The initial particle formation may be intensified by the raising the inhomogeneity of the mixture when retarding the injection timing from 30° CA BTDC to 20° CA BTDC. However, particle oxidation is promoted because of the higher temperature, as previously mentioned. It seems that particle oxidation is dominant during competition with particle formation.

Effect of the pilot mass on the combustion and the gaseous emissions

The effects of the pilot diesel mass on the combustion parameters are illustrated for the same injection timings in Figure 7. The increase in the pilot mass means that

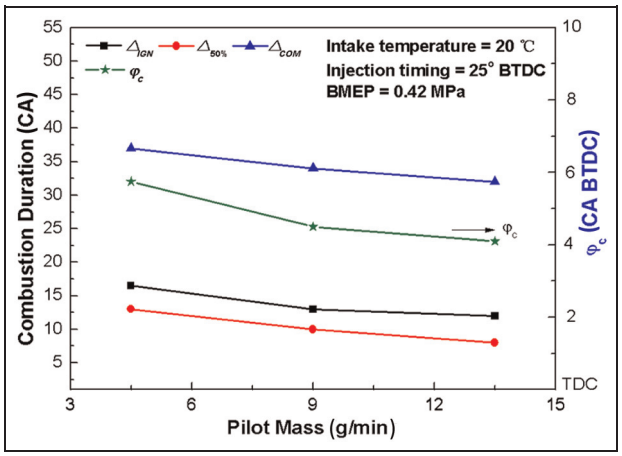

Figure 7. Combustion duration versus pilot mass at 1600 r/min engine speed.
CA: crank angle; BTDC: before top dead centre; BMEP: brake mean effective pressure; TDC: top dead centre.

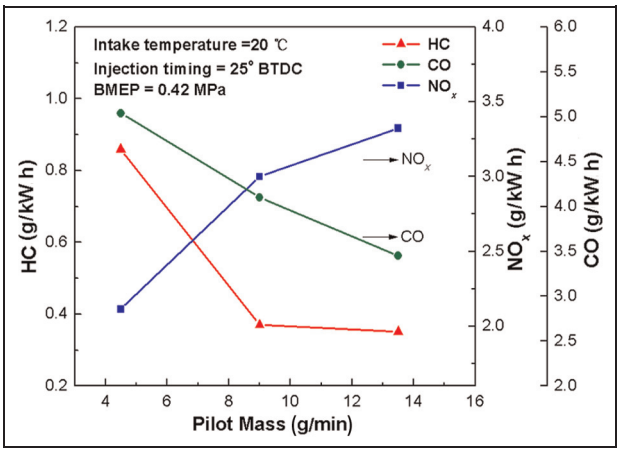

Figure 8. Exhaust HC, CO and NO_x emissions versus pilot mass at 1600 r/min engine speed.
BTDC: before top dead centre; BMEP: brake mean effective pressure; HC: hydocarbon; CO: carbon monoxide; NO_x: nitrogen oxides.

more and adequate ignition energy participates in combustion and causes an increase in the size of the high-temperature zones. Meanwhile, under the same load operation, the entire specific heat capacity of cylinder charge can be reduced relatively owing to the increase in the amount of natural gas. These two factors might jointly increase the cylinder temperature, shorten the diesel preparation time before ignition and effectively improve the initial burning rate. Therefore, with increasing pilot mass, Δ_{IGN} and Δ_{COM} continuously decrease and $\Delta_{50\%}$ increases slightly, while φ_c becomes gradually closer to the TDC.

Although a larger pilot mass can enhance the total in-cylinder temperature effectively, it yields some negative effects as well. Figure 8 shows the negative effects of increasing the pilot mass from 4.5 g/min to 13.5 g/min on gaseous emissions. It is a well-documented fact that increasing the pilot mass leads to higher NO_x and lower HC and CO emissions owing to the higher in-cylinder temperature and the fast burning rate.[13,19,34]

Effect of the pilot mass on the particulate matter emissions

Figures 9, 10 and 11 provide the particle number concentrations and the particle mass concentrations for various pilot injection quantities under different engine operation conditions. Like the analysis of the injection timing, consider, for example, particle emissions at an engine speed of 1600 r/min. As depicted in Figure 9, the particle number concentration decreases unexpectedly with increasing pilot mass. The peak particle number concentration occurs at a diameter of 0.039 μm as well, whereas the particle mass distribution curves shift upwards and towards a larger size with a peak at 0.2 μm in Figure 10. There are several reasons that might be responsible for such behaviour. First, under the same injection timings, a higher pilot diesel quantity favours the formation of larger particles. Meanwhile, the shorter Δ_{IGN} caused by the higher pilot mass yields an inhomogeneous mixture, which might further intensify the possibilities of forming larger particles and of decreasing the number of particles. Second, a higher pilot mass can generate a higher initial heat release rate and a higher in-cylinder temperature than a lower pilot mass can. Therefore, oxidation of the HC and particles is promoted, and thus the particle number concentration decreases unexpectedly. Third, the increased pilot mass virtually leads to a slight decrease in the total excess air ratio from 1.69 to 1.56 at a BMEP of 0.42 MPa, implying a slight reduction in the oxygen content in the cylinder. A higher temperature and decreasing oxygen availability might strengthen the particle coagulation rate to a certain degree. Hence, the number of larger particles is further increased and the particle mass concentration is increased with increasing pilot mass.

Conclusions

A single-cylinder diesel pilot NG-PCCI engine was used to investigate the impact of the diesel injection timing and the diesel pilot mass on the combustion and the emissions, especially the particle emissions. The results lead to the following conclusions.

1. The diesel injection timing directly affects the homogeneity of the diesel–natural-gas–air mixture, the ignition centre distribution and the ignition phase. Therefore, appropriately advancing the injection timing can prolong the ignition delay period, increase the homogeneity of charge, reduce the HC, CO and NO_x emissions and particle mass concentration and control the particle number concentration in a range.

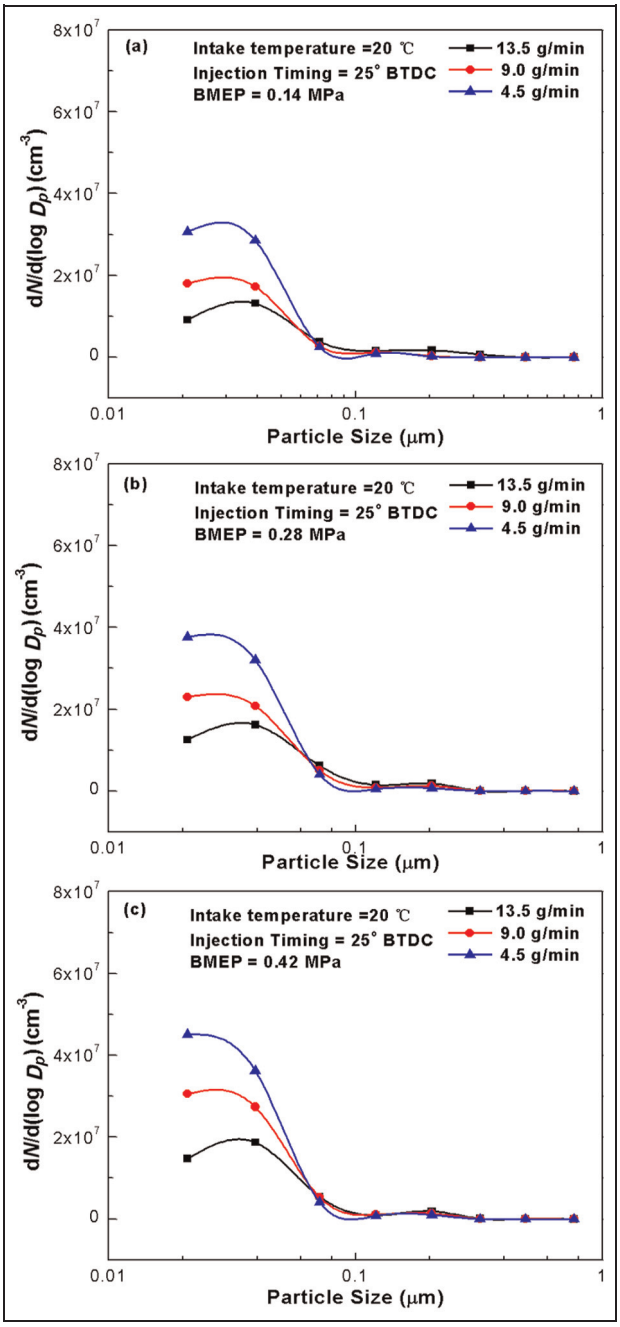

Figure 9. Particle number concentration with respect to the size distribution for various pilot masses at 1600 r/min engine speed.
BTDC: before top dead centre; BMEP: brake mean effective pressure.

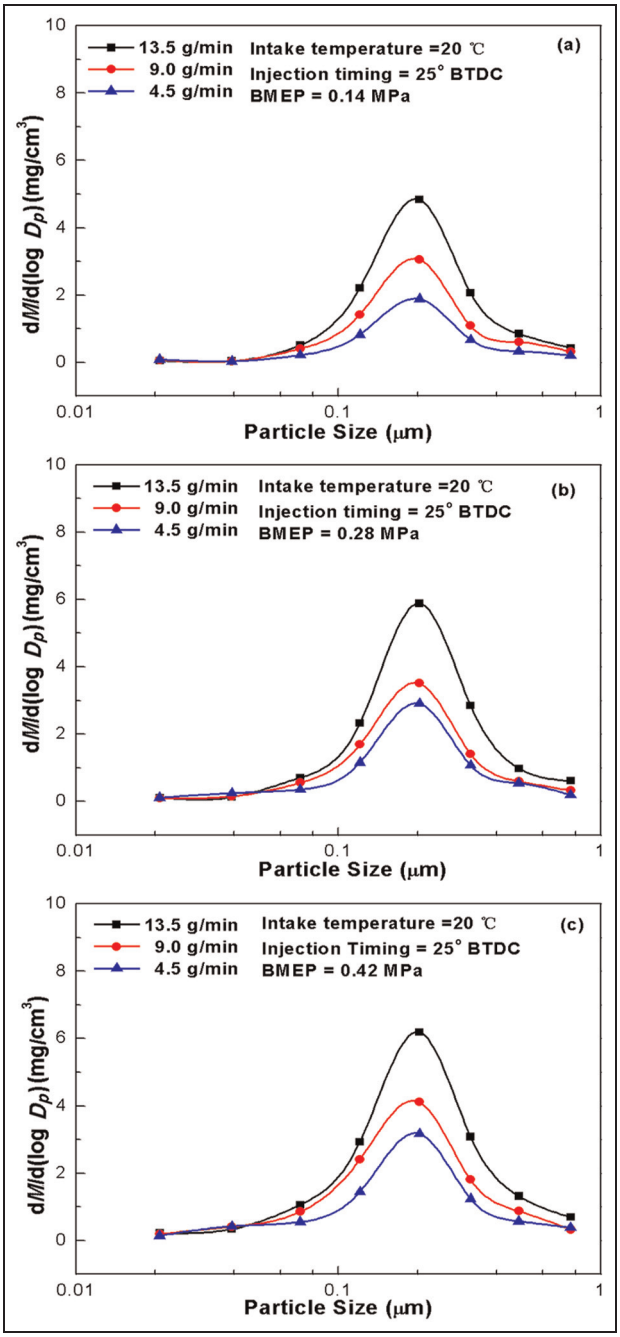

Figure 10. Particle mass concentration with respect to the size distribution for various pilot masses at 1600 r/min engine speed.
BTDC: before top dead centre; BMEP: brake mean effective pressure.

2. Increasing the pilot diesel mass can offer higher ignition energy and shorten the ignition delay period. These cause a higher in-cylinder temperature and poor homogeneity of the mixture. Both enhance the oxidation of particles and the formation of large particles respectively. As a result, the particle mass concentration is increased dramatically and the particle number concentration is decreased unexpectedly with increasing pilot mass. Meanwhile, the total HC and CO emissions are reduced and yet more NO_x emissions are produces as increasing the pilot mass.
3. The particles in a micro-diesel pilot NG-PCCI engine mainly consist of massive nanoparticles, and the peak particle diameter is near 0.039 μm. However, the particle mass is due mainly to the mass of the fine particles. The number of particles is more sensitive to the injection timing beyond 20° CA BTDC and is more sensitive when the pilot mass is less than the basic pilot mass. This offers a direction for optimizing the particle emissions by advancing the injection timing and increasing the pilot mass appropriately.

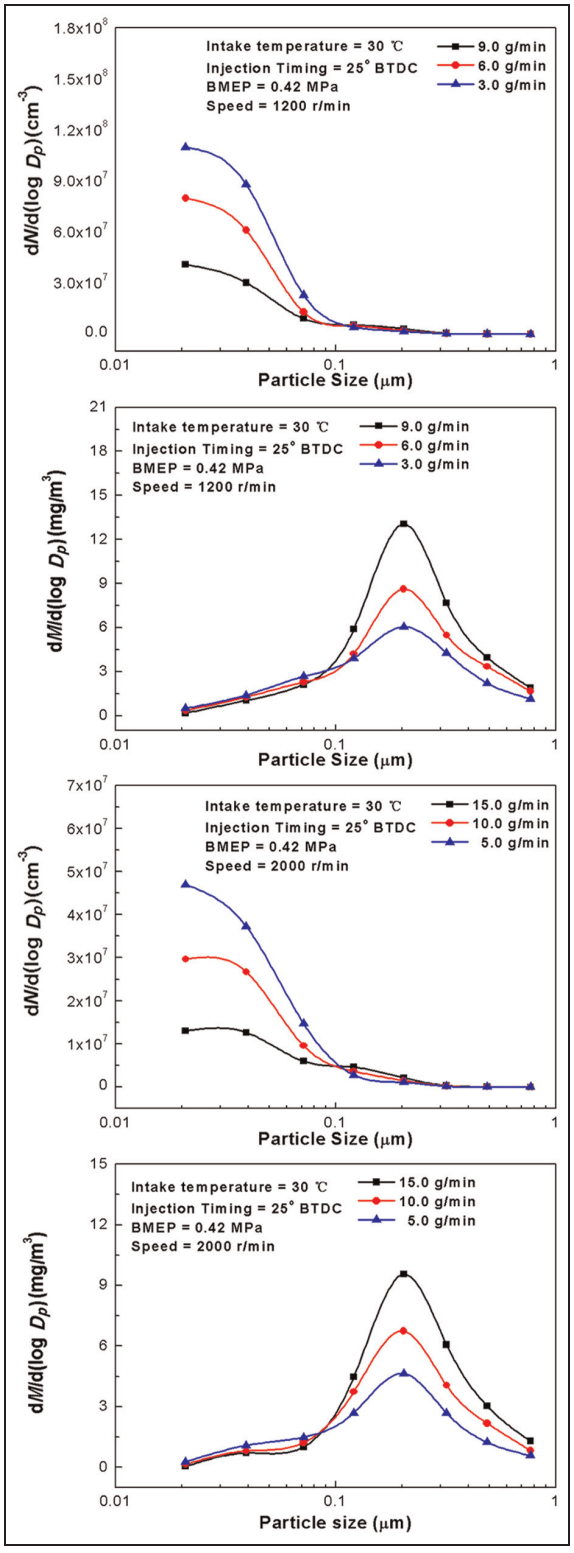

Figure 11. Particle number concentration and particle mass concentration for various pilot masses at 1200 r/min and 2000 r/min engine speeds.
BTDC: before top dead centre; BMEP: brake mean effective pressure.

Funding

This study is financially supported by the National Basic Program of China (Grant NO.2011CB707200).

References

1. McTaggart-Cowan GP, Rogak SN, Munshi SR and Hill PG. Combustion in a heavy-duty direct-injection engine using hydrogen–methane blend fuels. *Int J Engine Res* 2009; 10(1): 1–13.
2. Laforet CA, Brown BS, Rogak SN and Munshi SR. Compression ignition of directly injected natural gas with entrained diesel. *Int J Engine Res* 2010; 11(3): 207–218.
3. Olsson JO, Tunestål P, Johansson B et al. Compression ratio influence on maximum load of a natural gas fueled HCCI engine. SAE paper 2002-01-0111, 2002.
4. Kawasaki K, Hirota K, Nagata S et al. Improvement of natural-gas HCCI combustion by internal EGR by means of exhaust valve re-opening. SAE paper 2009-32-0079, 2009.
5. Jun D, Ishii K and Iida N. Combustion analysis of natural gas in a four stroke HCCI engine using experiment and elementary reactions calculation. SAE paper 2003-01-1089, 2003.
6. Handford DI and Checkel MD. Extending the load range of a natural gas HCCI engine using direct injected pilot charge and external EGR. SAE paper 2009-01-1884, 2009.
7. Papagiannakis RG and Hountalas DT. Combustion and exhaust emission characteristics of a dual fuel compression ignition engine operated with pilot diesel fuel and natural gas. *Energy Conversion Managmt* 2004; 45(18–19): 2971–2987.
8. Qi Y, Srinivasa KK, Krishnan SR et al. Effect of hot exhaust gas recirculation on the performance and emissions of an advanced injection low pilot-ignited natural gas engine. *Int J Engine Res* 2007; 8(3): 289–305.
9. Yao CD, Yao GT, Song JO and Wang YS. Mechanism on distribution of pilot fuel spray and compressing ignition in premixed natural gas engine ignited by pilot diesel. *Chin J Mech Engng* 2005; 18(1): 25–29.
10. Papagiannakis RG, Rakopoulos CD, Hountalas DT and Rakopoulos DC. Emission characteristics of high speed, dual fuel, compression ignition engine operating in a wide range of natural gas/diesel fuel proportions. *Fuel* 2010; 89(7): 1397–1406.
11. Krishnan SR, Srinivasan KK, Singh S et al. Strategies for reduced NO_x emissions in pilot-ignited natural gas engines. *Trans ASME, J Engng Gas Turbines Power* 2004; 126(3): 665–671.
12. Krishnan SR and Srinivasan KK. Multi-zone modelling of partially premixed low-temperature combustion in pilot-ignited natural-gas engines. *Proc IMechE Part D: J Automobile Engineering* 2010; 224(12): 1597–1622.
13. Srinivasan KK, Krishnan SR and Midkiff KC. Improving low load combustion, stability and emissions in pilot-ignited natural gas engines. *Proc IMechE Part D: J Automobile Engineering*, 2006; 220(2): 229–239.
14. Srinivasan KK, Krishnan SR, Singh S et al. The advanced injection low pilot ignited natural gas engine: a combustion analysis. *Trans ASME, J Engng Gas Turbines Power* 2006; 128(1): 213–218.
15. Srinivasan KK, Krishnan SR, Qi Y et al. Analysis of diesel pilot-ignited natural gas low-temperature combustion with hot exhaust gas recirculation. *Combust Sci Technol* 2007; 179(9): 1737–1776.

16. Donaldson K, Li XY and MacNee W. Ultrafine (nanometre) particle mediated lung injury. *J Aerosol Sci* 1998; 29(5–6): 553–560.
17. Pope CA. Epidemiology of fine particulate air pollution and human health: biologic mechanisms and who's at risk? *Environ Health Perspectives* 2000; 108: 713–723.
18. Kittelson DB. Engines and nanoparticles: a review. *J Aerosol Sci* 1998; 29(5–6): 575–588.
19. McTaggart-Cowan GP, Jones HL, Rogak SN et al. The effects of high-pressure injection on a compression-ignition, direct injection of natural gas engine. *Trans ASME, J Engng Gas Turbines Power* 2007; 129(2): 579–588.
20. Prikhodko VY, Curran SJ, Barone TL et al. Diesel oxidation catalyst control of hydrocarbon aerosols from reactivity controlled compression ignition combustion. In: *ASME 2011 international mechanical engineering congress and exposition*, Denver, Colorado, USA, 11–17 November 2011, paper IMECE2011–64147. New York: ASME.
21. Sahoo BB, Sahoo N and Saha UK. Effect of engine parameters and type of gaseous fuel on the performance of dual-fuel gas diesel engines – a critical review. *Renewable Sustainable Energy Rev* 2009, 13(6–7), 1151–1184.
22. Prikhodko VY, Curran SJ, Barone TL et al. Emission characteristics of a diesel engine operating with in-cylinder gasoline and diesel fuel blending. SAE paper 2010-01-2266, 2010.
23. Cha JP, Heo JY and Lee CS. Nanoparticle emissions of partial premixed charge compression ignition (PPCCI) engines at diesel–gasoline dual fuel combustion. In: *14th annual conference on liquid atomization and spray systems*, Jeju, Republic of Korea, 21–22 October 2010, pp. 47–52.
24. Liu YF, Liu B, Liu L et al. Combustion characteristics and particulate emission in a natural-gas direct-injection engine: effects of the injection timing and the spark timing. *Proc IMechE Part D: J Automobile Engineering* 2010; 224(8): 1071–1080.
25. Tsolakis A, Hernandez JJ, Megaritis A and Crampton M. Dual fuel diesel engine operation using H_2 center dot effect on particulate emissions. *Energy Fuels* 2005; 19(2): 418–425.
26. Maricq MM, Podsiadlik DH, Brehob DD and Haghgooie M. Particulate emissions from a direct-injection spark-ignition (DISI) engine. SAE paper 1999-01-1530, 1999.
27. Wang XG, Zheng B, Huang ZH et al. Performance and emissions of a turbocharged, high-pressure common rail diesel engine operating on biodiesel/diesel blends. *Proc IMechE Part D: J Automobile Engineering* 2011; 225(1): 127–139.
28. Mustafi NN and Raine RR. Electron microscopy investigation of particulate matter from a dual fuel engine. *Aerosol Sci Technol* 2009; 43(9): 951–960.
29. Heywood JB. *Internal combustion engine fundamentals*. New York: McGraw-Hill, 1988.
30. Woschni G. A universally applicable equation for the instantaneous heat transfer coefficient in the internal combustion engine. SAE paper 670931, 1967.
31. Gordon S and McBride BJ. Computer program for calculation of complex chemical equilibrium compositions and applications. 1. Analysis. Reference Publication NASA RP-1311, National Aeronautics and Space Administration, Washington, DC, USA, 1994.
32. McBride BJ and Gordon S. Computer program for calculation of complex chemical equilibrium compositions and applications 2. User's manual and program description. Reference Publication NASA RP-1311-P2, National Aeronautics and Space Administration, Washington, DC, USA, 1996.
33. De Ojeda W, Zoldak P, Espinosa R and Kumar R. Development of a fuel injection strategy for partially premixed compression ignition combustion. SAE paper 2009-01-1527, 2009.
34. Papagiannakis RG, Hountalas DT and Rakopoulos CD. Theoretical study of the effects of pilot fuel quantity and its injection timing on the performance and emissions of a dual fuel diesel engine. *Energy Conversion Managmt* 2007; 48(11): 2951–2961.

Appendix 1

Notation

A	wall area (m^2)
C_p	specific heat at constant pressure (J/kg K)
C_V	specific heat at constant volume (J/kg K)
$dp/d\theta$	rate of pressure rise with respect to the crank angle
$dQ_B/d\theta$	heat release rate with respect to the crank angle
$dQ_w/d\theta$	heat transfer rate with respect to the crank angle
h_c	heat transfer coefficient (J/m^2 s K)
m	mass of in-cylinder gases (kg)
R	gas constant (J/kg K)
T	mean gas temperature (K)
T_w	wall temperature (K)
V	cylinder volume (m^3)
Δ_{COM}	crank angle for the total combustion duration
Δ_{IGN}	crank angle for the ignition delay period
$\Delta_{50\%}$	crank angle for the 50% mass fraction burned
φ_c	crank angle at the centre of heat release
φ_e	crank angle at the end of heat release
φ_s	crank angle at the beginning of heat release

Abbreviations

BTDC	before top dead centre
CA	crank angle
NG-HCCI	natural-gas homogeneous charge compression ignition
NG-PCCI	natural-gas premixed charge compression ignition
TDC	top dead centre